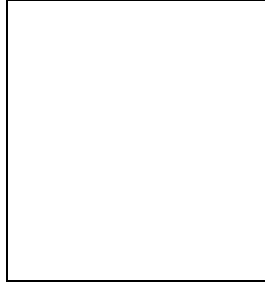# CHARM IN ELECTRON–PROTON COLLISIONS

A. BERTOLIN

on behalf of the ZEUS and H1 collaborations

Istituto Nazionale di Fisica Nucleare, Sezione di Padova

Via Marzolo 8, 35131 Padova, Italy

Charm in electron–proton collisions is a particularly large and interesting field. For this summary two topics particularly relevant for HERA have been selected. First the study of inelastic J/ψ production in both the photoproduction and the electroproduction regime, study still needed to clarify the J/ψ production mechanisms. Second the analysis of $D^\star$ photoproduction events, study than can lead to a better understanding of the photon structure.

1 Inelastic J/ψ photoproduction

The inelastic J/ψ photoproduction process has been measured by both the H1 [1] and ZEUS [2] collaborations. The key variable describing this process is the inelasticity, z. In the proton rest frame z is the fraction of the virtual photon energy taken by the J/ψ. Resolved photon processes are expected to dominate at low z while for $0.2 \leq z \leq 0.9$ direct photon processes take over and hence the characteristic inelasticity shape shown in the top left plot of fig. 1 by the LO calculation labelled KZSZ (LO,CS+CO). The production at higher z values is ascribed to diffractive processes. Two different categories of subprocesses contribute to the direct and to the resolved part, called colour singlet, CS, and colour octet, CO, processes. The introduction of the CO component is a consequence of non relativistic QCD theories and is needed to explain the magnitude of the J/ψ cross section seen by CDF. The HERA data shown in the top left plot of fig. 1 are consistent with these prediction although the rise of the inelasticity cross section for $z \gtrsim 0.6$ is softer in the data with respect to the KZSZ (LO,CS+CO) prediction. The H1 data for $z \gtrsim 0.4$ have been scaled to take into account a small difference in the W integration range between the ZEUS and the H1 analyses. The low z H1 data, $z \lesssim 0.4$, are integrated for $120 < W < 260$ GeV. The different W integration range is not taken into in the data or the theoretical predictions. The measured inelasticity differential cross section is also compared to a

NLO calculation including only the direct photon colour singlet process, KZSZ (NLO,CS). This calculation, available only for $0.2 < z < 0.9$, describes, within large theoretical uncertainties, both the shape and the normalization of the data. The same calculation can also account for the p_T^2 differential cross section, as shown by the top right plot of fig. 1. In the HERA case the NLO corrections to the direct photon colour singlet process are found to be large and increasing with p_T^2, as can be seen by comparing the LO and NLO predictions.
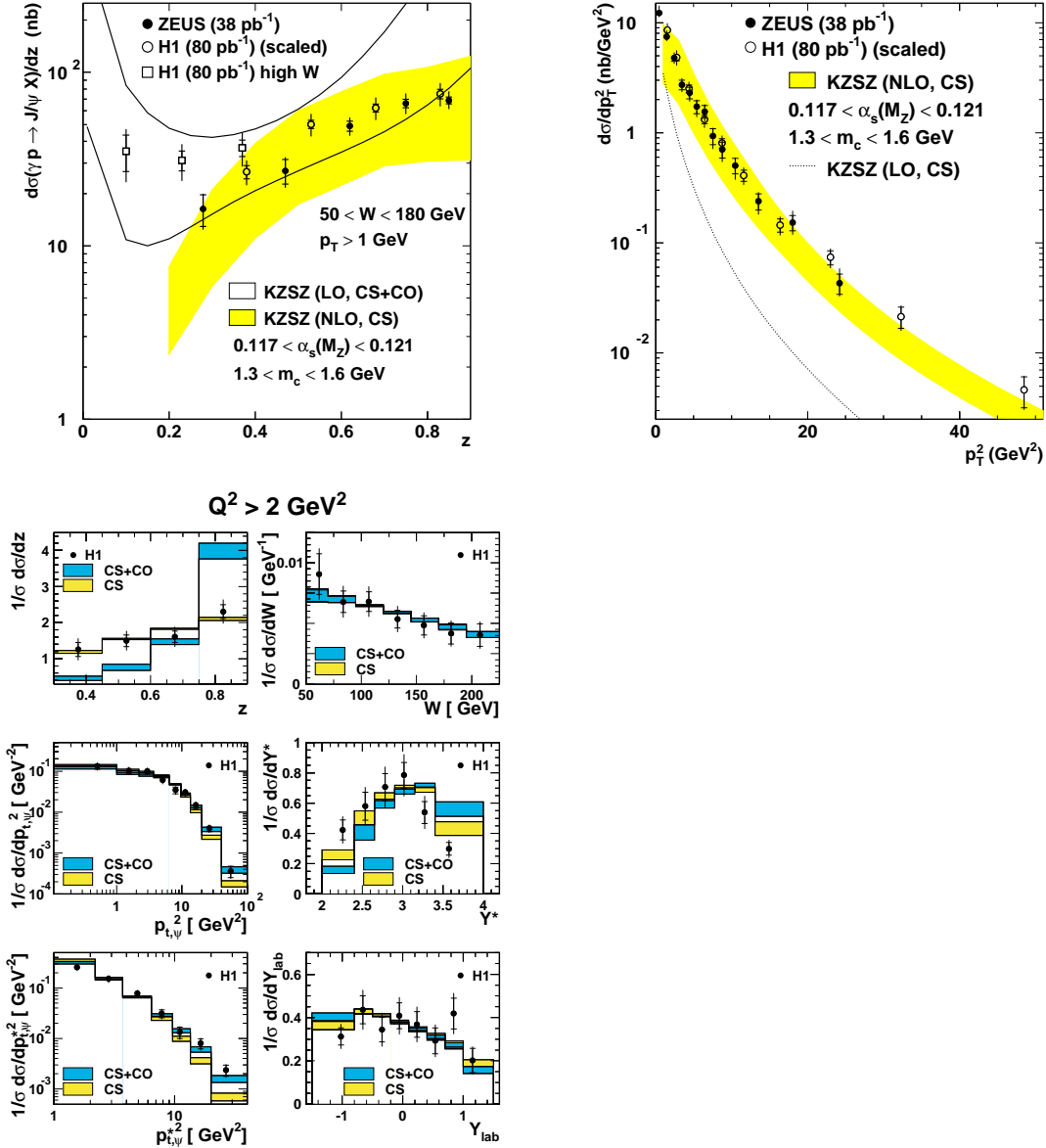

Figure 1: Inelasticity, z, upper left, and p_T^2, upper right, differential cross section measured by the ZEUS and H1 collaborations for the inelastic J/ψ photoproduction process. The theoretical predictions are described in the text. The bottom left plot shows the inelasticity, z, photon proton center of mass energy, W, J/ψ transverse momentum squared, $p_{t,\psi}^2$, J/ψ rapidity in the $\gamma^\star p$ frame, $Y^\star$, J/ψ transverse momentum squared in the $\gamma^\star p$ frame, $p_{t,\psi}^{\star 2}$ and J/ψ rapidity in the lab. frame, Y_{lab}, differential cross sections measured by the H1 collaboration for the inelastic J/ψ electroproduction process. The theoretical predictions are described in the text.

2 Inelastic J/ψ electroproduction

The inelastic J/ψ process in the high Q^2 regime, the electroproduction regime, has been measured by the H1 collaboration [3]: the inelasticity, z, photon proton center of mass energy, W, J/ψ transverse momentum squared, $p^2_{t,\psi}$, J/ψ rapidity in the $\gamma^\star$ p frame, $Y^\star$, J/ψ transverse momentum squared in the $\gamma^\star$ p frame, $p^{\star 2}_{t,\psi}$ and J/ψ rapidity in the lab. frame, Y_{lab}, are shown in bottom left series of plots in fig. 1 [a]. The data are compared to a LO calculation including the CS component only, identified by the label CS, or including both the CS and the CO component, CS+CO. To avoid the large normalization uncertainties of a LO calculation only the shapes of the various distributions are considered. As in the photoproduction case, the key variable is the inelasticity, z: the shape measured in the data clearly favor the CS component only hypothesis.

3 $D^\star$ photoproduction

$D^\star$ photoproduction has been investigated in detail by the ZEUS collaboration [4]. Measurements of the $D^\star$ transverse momentum, $p_T(D^\star)$, $D^\star$ pseudorapidity, $\eta(D^\star)$, photon proton center of mass energy, W, and $D^\star$ inelasticity, z, differential cross sections are shown in the left part of fig. 2. The data are compared to a NLO QCD calculation, identified by the label NLO QCD, and to a calculation incorporating mass effects up to the NLO and resuming p_T logarithms up to the NLL level, labelled FONLL, available only for fig. 2 (a) and (b). The NLO QCD calculation can describe the data in the forward region and at low z values only using extreme values for the non perturbative input parameters ($m_c = 1.3$ GeV). Instead for $0.6 < z < 1$, see fig. 2 (d), the normalization of the NLO QCD prediction matches the data. It can be shown that this region corresponds mostly to the direct photon process.
In $D^\star$ events with two hadronic jets the separation between direct and resolved photon processes can also be achieved using the variable x_γ^{obs} defined as:

$$x_\gamma^{obs} = \frac{\Sigma_{jets} E_t^{jet} e^{-\eta^{jet}}}{2 y E_e}$$

where E_t^{jet} and η^{jet} are the transverse energies and the pseudorapidities of the two jets, respectively, E_e is the electron beam energy and y, in the proton rest frame, is the fraction of the electron energy take by the quasi–real exchanged photon. Direct and resolved photon events are selected by requiring x_γ^{obs} to be above or below the threshold value of 0.75, respectively. The right part of fig. 2 shows the $\cos\theta^\star$ differential cross section, where $\theta^\star$ is the angle between the jet–jet axis and the proton–photon axis in the parton–parton rest frame, for direct and resolved photon events. This distribution should behave like:

$$d\sigma/d|\cos\theta^\star| \approx (1 - |\cos\theta^\star|)^{-2S}$$

where S is the spin of the exchanged propagator.

The data for $x_\gamma^{obs} < 0.75$, the resolved photon region, show a steeper rise of the cross section in the photon direction with respect to the $x_\gamma^{obs} > 0.75$ selection, the direct region. Hence gluon exchange is the dominant mechanism in the $x_\gamma^{obs} < 0.75$ region. Furthermore since the charm jet is close to the photon in rapidity charm must come from the photon. This class of diagrams, called charm flavour excitation in the photon, are implemented in the PYTHIA MC which describes the $\cos\theta^\star$ differential cross section for both x_γ^{obs} selections. The HERWIG MC gives also a good description of the data for $x_\gamma^{obs} > 0.75$ but is worse than PYTHIA for $x_\gamma^{obs} < 0.75$. In the CASCADE MC the k_T unintegrated gluon density of the proton obey the CCFM evolution equation. In this case even if the CASCADE matrix elements correspond to the direct photon process only resolved photon processes are reproduced by the CCFM initial state radiation. CASCADE fails to reproduce the data for $x_\gamma^{obs} > 0.75$ but gives a good description of

---

the data for the lower x_γ^{obs} range. A NLO QCD calculation, including hadronization corrections, identified by the label NLO QCD ⊗ HAD, gives a good description of the data for $x_\gamma^{obs} > 0.75$ but is only marginally consistent with the data for $x_\gamma^{obs} < 0.75$ in the photon direction.
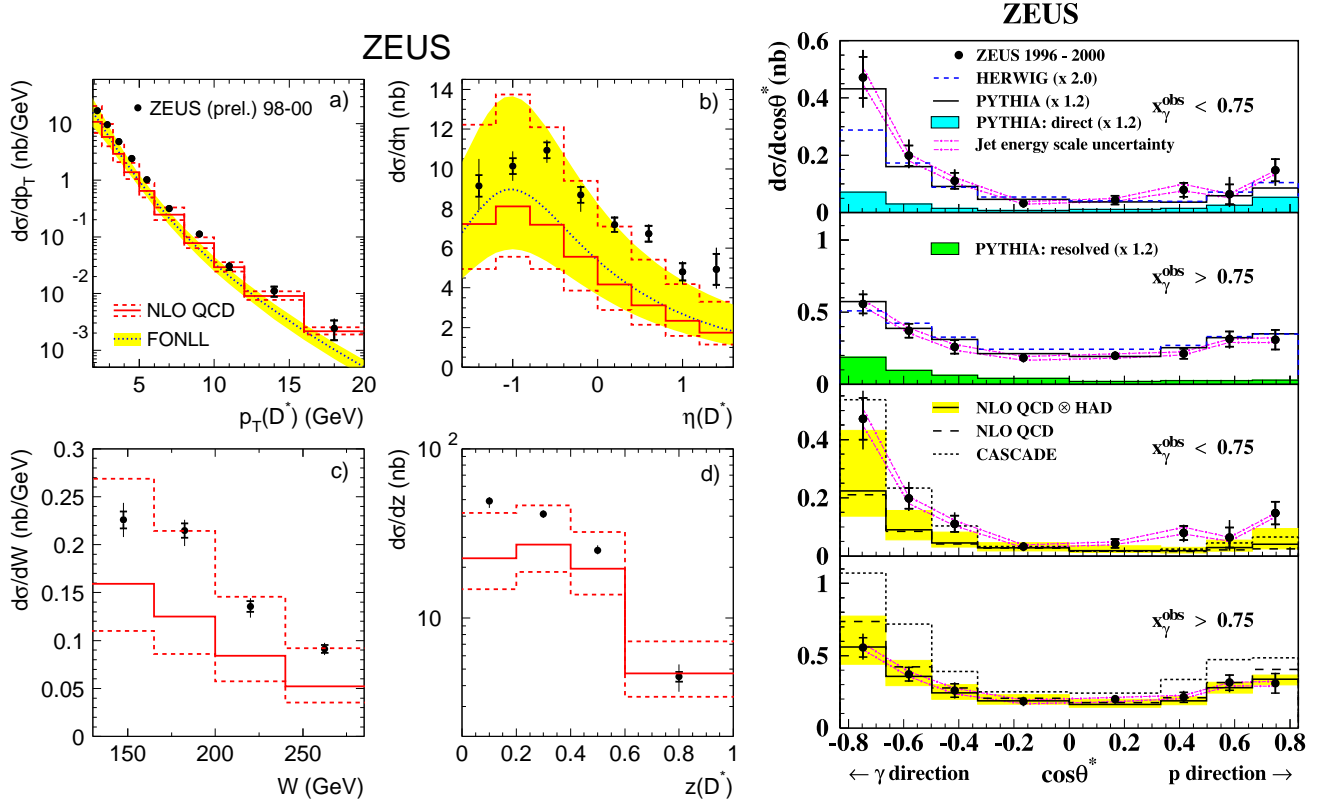

Figure 2: Measurements of the $D^\star$ transverse momentum, $p_T(D^\star)$, $D^\star$ pseudorapidity, $\eta(D^\star)$, photon proton center of mass energy, W, and $D^\star$ inelasticity, z, differential cross sections are shown in fig. from (a) to (d), respectively. The right side compares the $\cos\theta^\star$ differential cross section, where $\theta^\star$ is the angle between the jet–jet axis and the proton–photon axis in the parton–parton rest frame, for two different x_γ^{obs} selections, to MC models and QCD predictions. All models and predictions are described in the text.

References

1. C. Adloff *et al*, *Eur. Phys. J.* C **25**, 25 (2002).
2. S. Chekanov *et al*, *Eur. Phys. J.* C **27**, 173 (2002).
3. C. Adloff *et al*, *Eur. Phys. J.* C **25**, 41 (2002).
4. S. Chekanov *et al*, DESY-03-015, submitted to *Phys. Lett.* B;
   S. Chekanov *et al*, Abstract 786 Submitted to the XXXIst International Conference on High Energy Physics, 24-31 July 2002, Amsterdam, The Netherlands.